Chemical Physics 88 (1984) 17–25
North-Holland, Amsterdam

COLLISION DYNAMICS OF NON-INTEGRABLE SYSTEMS: VALIDITY OF CLASSICAL SCALING

Ramakrishna RAMASWAMY

Tata Institute of Fundamental Research, Homi Bhabha Road, Bombay 400 005, India

Received 30 December 1983

The classical collision dynamics of a model atom–molecule non-integrable collision system is studied, and the energy transfer (ET) moment is examined as a function of the initial semiclassical level of the molecule. A recently derived classical scaling theory is shown to be valid in the case when the molecular motion remains regular throughout the collision, and the ET variation is then characterized by a polynomial dependence on the initial (semiclassical) quantum numbers. When chaotic motions participate, the ET no longer follows the scaling law. The utility of the scaling theory in providing the proper interpolation form for extending classical trajectory data in non-integrable collision systems is discussed.

1. Introduction

Non-integrable hamiltonian dynamical systems have been studied in a variety of applications to chemical problems [1,2]. One area of interest is in modeling (externally perturbed) evolving systems – as in bimolecular collision [3–7] or multiphoton absorption [8] phenomena. A general conclusion that has emerged from some recent studies is that classically there are two different dynamical behaviours, which can be considered the reflection of quasiperiodic (toroidal) and aperiodic (chaotic) motions in conservative non-integrable hamiltonian systems [1,2,9,10].

An example is afforded by an atom–molecule collision system, for which the overall classical hamiltonian is

$$H = T + V(R, q) + H_0(p, q). \qquad (1)$$

Here R is the collision coordinate, $T = p_R^2/2\mu$ the relative kinetic energy, p_R the relative momentum and μ is the reduced mass. The molecular hamiltonian H_0 is chosen to be non-integrable in N degrees of freedom; in usual notation, the momenta and coordinates are denoted p and q. At $t = t_0$ and $t \to \infty$, i.e. at the beginning and end of the collision, $R \to \infty$ and $V \to 0$. Then T and H_0 are conserved quantities although during the collision these change. (For purposes of clarity, "orbit" will denote the internal motion of H_0 viewed separately, and "trajectory" will refer to the overall motion of hamiltonian (1).)

For problems such as above, scaling laws [11,12] have been derived in recent work. This classical scaling theory (CST) relates the variation of arbitrary dynamical quantities with certain initial conditions through simple polynomial expressions. Earlier applications [11,13–15] of the CST have been to asymptotically integrable collision systems. The expressions used there related the variation of vibrational-phase-averaged energy transfer (ET) with the initial action variable (for molecular situations it is customary to work in action–angle coordinates since actions can be identified with quantum numbers). There are two principal advantages in using the CST. Firstly, the use of a scaling formula greatly reduces computational effort, since it offers a means of accurate prediction by providing the correct interpolation *and* extrapolation form. Further, analysis of the scaling coefficients in terms of quantum transition probabilities is possible in some cases, and this affords an (at least qualitative) understanding of quantum effects from a small number of classical trajectories. Both facets of the CST have been exploited in previous work [14,15].

0301-0104/84/$03.00

The realistic modeling of chemical situations involves non-integrable systems, and it would be advantageous to establish the regime of applicability of the CST in such cases as well. The dynamical variables studied here are average energy transfer moments, $[H_0(t=\infty)-H_0(t=t_0)]^k$, $k=1, 2\ldots$, as a function of the initial semiclassical state in the collision dynamics of a collinear atom–triatom system. Thus H_0 is non-integrable in $N=2$ degrees of freedom. The semiclassical quantization [2,16] is effected by the usual EBKM rules, by locating particular tori $\Sigma_{n_1 n_2}$ for which the action integral

$$I_i = \oint_{C_i} \boldsymbol{p}\cdot \mathrm{d}\boldsymbol{q}, \quad i=1,2 \tag{2}$$

equals $(n_i+\alpha_i/4)h$ where n_i are integers and α_i the Maslov indices along the independent paths C_i on the torus. By the correspondence principle [16], the invariant torus $\Sigma_{n_1 n_2}$ is the semiclassical analogue of the quantum eigenstate $n_1 n_2$.

In geometric terms, for an integrable, one-degree-of-freedom system, the initial state is classically represented as an invariant circle in the phase plane. The final state is also a circle, but is usually *not* invariant (and corresponds to a quantum non-stationary state). For two degrees of freedom, the initial state is the invariant torus, $\Sigma_{n_1 n_2}$. In contrast to the previous situation, there are three possible outcomes of the evolution of this torus when the system is non-integrable. The final state can be a (non-stationary) (i) quasiperiodic state, (ii) chaotic state or (iii) a mixture of these. For all initial conditions on Σ, in case (i) or (ii), *all* final conditions lead to either quasiperiodic or chaotic orbits of H_0 respectively; in case (iii), the final conditions for some trajectories correspond to quasiperiodic orbits of H_0, and others to chaotic orbits.

A pictorial representation of the possible internal behaviour along a trajectory is shown in fig. 1. We focus on the molecular hamiltonian, and consider the motion of the orbit through the phase space of H_0. The initial orbit is quasiperiodic. Up to the interaction region $t_1 < t < t_2$, there is little change in the internal motion, which continues to be on a torus. In passing through the interaction region, the trajectory can force the orbit to (A) pass through only regular regions such that the final orbit is regular, or pass from the regular to the chaotic part of the internal phase space. There are two further possibilities here, (B) the orbit can then return to the regular region so that the final motion is regular, or (C) it can continue in the chaotic region, so that one has a final chaotic orbit. Thus all trajectories being of type (A) or (B) lead to a final quasiperiodic state and all of type (C) to a final chaotic state.

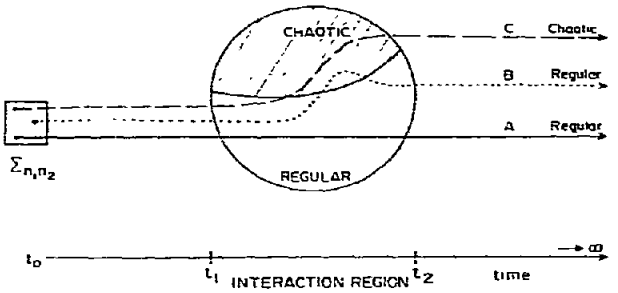

Fig. 1. Schematics of the possible internal motion during the collision. The interaction region is the time interval during which $\partial H_0/\partial t$ is sufficiently different from zero.

The interest in some earlier collision studies [3,4,7] has been in contrasting the dynamics deriving from (initial) toroidal versus chaotic orbits. Noid and Koszykowski [3] found, for example, that the behaviour of the (microcanonically averaged) energy transfer moment differed depending on whether the motion was largely regular or largely chaotic. In a more recent and detailed study, Nalewajski and Wyatt [7] have examined particular orbits rather than averages, and find good examples of (A) and (C) trajectories, and their reverse, and also of initial conditions on a chaotic orbit leading to regular or chaotic final conditions. They note [7] that there is a weak propensity for an initial regular (chaotic) orbit to evolve into a final regular (chaotic) orbit, and have termed this a hysteresis effect. In an similar study (where H_0 was taken as the Hénon–Heiles hamiltonian) Schatz [4] examined the energy transfer as a function of particular initial conditions at fixed initial internal energy. No *qualitative* difference was seen in going from low energies (where the motion in H_0 is largely regular) to higher energies (when chaos predominates). Some of these conclu-

sions have a bearing on the present study, and will be discussed later.

In this paper we restrict attention to the question of the validity of the scaling law. Due to the three possibilities in the collisional evolution identified above, there is a fundamental difference between integrable and non-integrable cases, and the primary observation is that the classical scaling behaviour is reliably followed *only* when the internal motion stays regular throughout the collision. The details of the system are briefly given in section 2. It is straightforward to apply the CST to the computed moments; of greater interest are the cases where it breaks down. These results are given in section 3, and a summary follows in section 4.

2. System and scaling form

The model non-integrable "molecular" hamiltonian chosen is

$$H_0(\boldsymbol{p}, \boldsymbol{q}) = \left(p_1^2 + p_2^2 + a_1 q_1^2 + a_2 q_2^2 \right)/2 + \lambda q_1 q_2^2, \tag{3}$$

which has been studied extensively [17–19] for the parameter values $a_1 = 1.6$, $a_2 = 0.9$, $\lambda = -0.08$. It is convenient to use these values here since tori Σ_{nm} corresponding to a number of semiclassical states of this system (with $\hbar = 1$) have already been specified [17]. (The initial condition is given in terms of a parameter f_2 which yields the momenta p_1, p_2 at the point $q_1 = q_2 = 0$ on the torus.) The validity of the CST is independent of the form of the interaction potential, here taken as an exponential repulsion,

$$V(R, \boldsymbol{q}) = \exp\left[-\alpha(R - q_1 - q_2) \right]. \tag{4}$$

The features of the dynamics are, however, very sensitive to the actual form of the potential. We choose the form above in order to avoid complications due to long-lived sticky collisions which can occur when $V(R, \boldsymbol{q})$ has an attractive part.

The average energy transfer is the change in H_0,

$$\begin{aligned} \mathrm{ET}(n_1, n_2) &= \langle H_0(t = \infty) - H_0(t = t_0) \rangle \\ &= -\langle T(t = \infty) - T(t = t_0) \rangle. \end{aligned} \tag{5}$$

$\langle\ \rangle$ denotes an average over several trajectories, initial conditions for which uniformly sample the invariant torus $\Sigma_{n_1 n_2}$ at initial time t_0, at fixed initial relative kinetic energy $E_k = T(t_0)$. Averages of higher-order moments of the ET or other dynamical quantities are similarly defined. The variation of the ET is described by a polynomial form

$$\mathrm{ET}(n_1, n_2) = \sum_{i,j} \gamma_{ij} n_1^i n_2^j = \sum_{ij} \bar{\gamma}_{ij} I_1^i I_2^j, \tag{6}$$

where the n_i are the (semiclassical) quantum numbers and the I_i are the actions defined via eq. (2). The scaling coefficients γ, $\bar{\gamma}$ naturally depend on E_k. For a sequence of states, when n_1 or n_2 is fixed, eq. (6) reduces to a polynomial in a single quantum number (or action). For integrable systems it is possible [11,12] to derive a scaling law at a given time for a particular vibrational phase. For non-integrable systems it is simpler (and safer) to study the scaling of phase-averaged quantities. The difficulty is that the initial conditions derived from f_2 can correspond to widely disparate initial angles (conjugate to the actions defined by eq. (2)) on the tori $\Sigma_{n_1 n_2}$. In particular, the dependence of the ET on f_2 at a fixed value of the initial internal energy, $H_0(t = t_0)$, will not necessarily be smooth even if all f_2 correspond to toroidal motion (see ref. [4]).

3. Results

We recall a few features of the isolated system described by H_0 (with $a_1 = 1.6$, $a_2 = 0.9$, $\lambda = -0.08$). The dissociation energy is 25.3125 units, and classical chaos becomes widespread above the energy of $E_c \approx 19$ units [17,19]. The semiclassical quantization is discussed in ref. [17]. The two sequences of states studied here (some relevant details are given in table 1) are $\{n_1, n_2 = 0\}$, $\{n_1 = 10, n_2\}$. By referring the f_2 values in table 1 to the Poincaré surfaces of section (PSS) in ref. [17], it can be seen that the states $\{n_1, 0\}$ are associated with extremely stable tori, whereas tori for $\{10, n_2\}$ states are located *near* regions of widespread chaos at the higher energies.

Moments of the energy transfer are computed for the collision system, eqs. (1), (3) and (4), for three values of the initial kinetic energy (here in arbitrary reduced units) $E_k = 0.5$, 1 and 2, for the

Table 1
Semiclassical energies and initial conditions of sequences of states for the molecular hamiltonian (3), with $a_1 = 1.6$, $a_2 = 0.9$, $\lambda = -0.08$ (taken from ref. [17])

n_1	n_2	$E_{n_1 n_2}$	$f_2(n_1 n_2)$
0	0	1.1051	0.4171
1	0	2.3673	0.1847
2	0	3.6296	0.1138
6	0	8.6786	0.0380
8	0	11.2032	0.0263
12	0	16.2522	0.0144
10	2	15.4952	0.0818
10	4	17.2350	0.1271
10	6	18.9448	0.1601
10	8	20.6209	0.1849
10	10	22.2602	0.2059
10	12	23.8654	0.2361

two sequences of levels. The remaining parameters in the collision hamiltonian and the potential are set at $\mu = 1$ and $\alpha = 0.5$; the results of this computation are presented in fig. 2 and tables 2 and 3.

3.1. Application of the CST

Given j data points (here values of the ET moment), one can always fit an mth-order ($m < j$) polynomial to these, or pass a unique jth-order polynomial through these points. What distinguishes a scaling behaviour from curve-fitting is the gradual *convergence* of the coefficients (such as γ in eq. (6)) in the polynomial as the number of data points and the order of the polynomial is increased. The convergence can easily be demonstrated when there is a large amount of input

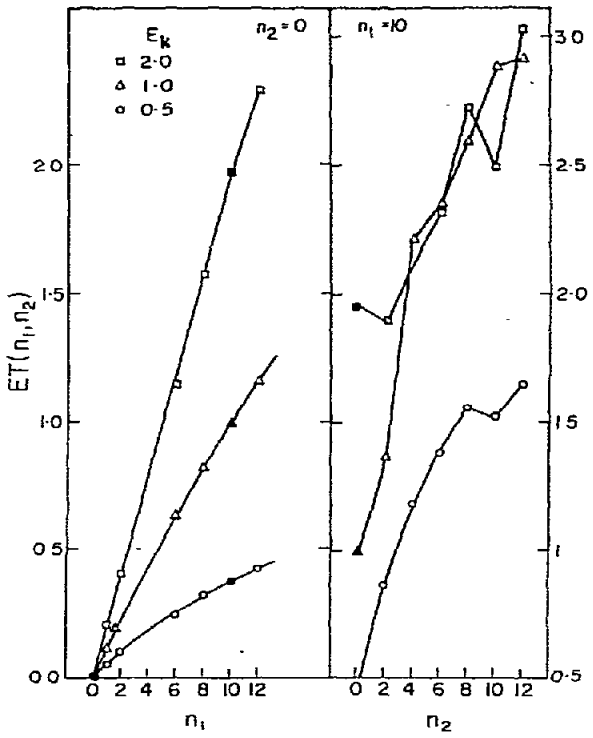

Fig. 2. ET moment versus initial semiclassical state for the two sequences of levels studied. Where there is no discernible scaling behaviour, the various data points are joined by straight lines. Open symbols correspond to computed moments, and the filled symbols to scaled moments.

Table 2
Exact and scaled ET for the sequence of states $\{n_1, 0\}$. Since n_2 is fixed for all states, the scaling form is a polynomial in n_1

n_1	$E_k = 0.5$		$E_k = 2.0$	
	exact $ET(n_1, 0)$	scaled values	exact $ET(n_1, 0)$	scaled values
0	−0.959(−2) [b]	input	0.316(−1)	input
1	−0.560(−1)	input	−0.205	input
2	−0.103	−0.985(−1)	−0.404	−0.395
6	−0.240	input	−1.149	input
8	−0.326	−0.300	−1.576	−1.587
10	n.a. [a]	−0.370	n.a.	−2.010
12	−0.428	input	−2.286	input

[a] f_2 for this level not given in ref. [17].
[b] Here and elsewhere in the tables, $x(-m) = x \times 10^{-m}$.

Table 3
Exact and scaled ET for the sequence of states $\{10, n_2\}$ at $E_k = 0.5$

n_2	Exact ET(10, n)	Scaled values
0	n.a.	−0.391
2	−0.861	input
4	−1.178	−1.172
6	−1.383	input
8	−1.555	input
10	−1.520	−1.747
12	−1.641	−2.020

information (e.g. ref. [14]); here we are limited by the small number of states within any sequence. However, the data given in tables 4–6 are representative of the cases where one can discern the presence or absence of proper scaling behaviour. When successive data points do not lie on a smooth (low-order polynomial) curve, then the coefficients change erratically (tables 5 and 6). For a small set of input data, this is one indication of a departure from the CST.

The variation of the ET for the sequence $\{n_1, 0\}$ is well described in a *three-term* scaling formula at all kinetic energies. For oscillator systems like (3), these states are also the most "harmonic" and the near-linear variation of the ET is typical [11,15]. In table 4 the convergence behaviour of the coefficients is shown at $E_k = 2.0$. It is clear that the

Table 4
Convergence characteristics of the first three coefficients [a] for the sequence $\{n_1, 0\}$ at $E_k = 2.0$. In addition to the exact moments in table 2 ,the moment ET(−1/2, 0) = 0.140 is included as input

n_1 [b]	β_0	β_1	β_2
−1/2	0.140		
0	0.136(−1)	−0.253	
1	0.136(−1)	−0.241	0.228(−1)
2	0.136(−1)	−0.239	0.254(−1)
6	0.136(−1)	−0.238	0.257(−1)
8	0.136(−1)	−0.238	0.258(−1)
12	0.136(−1)	−0.237	0.259(−1)

[a] The scaling expression used is $ET(n_1, 0) = \Sigma_m \beta_m n_1^m$.
[b] The rows are indexed here by n_1 to show how the β change as ET(n_1, 0) is added in the input set and the order of the polynomial is increased by one.

Table 5
Convergence behaviour of the coefficients [a] for the sequence $\{10, n_2\}$ at $E_k = 0.5$. In addition to the data in table 3, we include ET(10, −1/2) = −0.242

n_2 [b]	β_0	β_1	β_2
−1/2	−0.242		
2	−0.366	−0.247	
4	−0.386	−0.277	0.178(−1)
6	−0.389	−0.281	0.247(−1)
8	−0.387	−0.279	0.214(−1)
10	−0.373	−0.266	−0.215(−2)
12	−0.330	−0.230	−0.793(−1)

[a] The scaling expression used is $ET(10, n_2) = \Sigma_m \beta_m n_2^m$.
[b] The rows are indexed here by n_2 to show how the β change as ET(10, n_2) is added in the input set and the order of the polynomial is increased by one.

various moments do indeed lie on a smooth curve, and the predictive accuracy (table 2) is reasonably good. From these data we can determine ET(n_1, 0) even if $\Sigma_{n_1 0}$ is not known: hence for *all* states $n_1 \leqslant 12$, $n_2 = 0$.

In contrast, for the sequence $\{10, n_2\}$ the ET variation does not seem to follow any simple pattern at $E_k = 1$ and 2. At the lowest kinetic energy, however, the ET from levels with $n_2 \leqslant 8$ lie on a smooth curve, quite different from the moments from $n_2 = 10$ and 12 (see fig. 2). In table 5 the coefficients deriving from the first 5 input moments appear to be converging; however the variation in the coefficients as the last two points are added signifies that these do not follow the same pattern as the others. (This is merely a quantitative

Table 6
Behaviour of the coefficients [a] for the sequence $\{10, n_2\}$ at $E_k = 2.0$

n_2 [b]	ET(10, n_2)	β_0	β_1	β_2
2	−1.362	−1.362		
4	−2.214	−0.510	−0.426	
6	−2.344	−0.212	−0.968	0.903(−1)
8	−2.596	1.056	−1.741	0.301
10	−2.887	1.983	−2.707	0.639
12	−2.918	2.694	−3.517	0.972

[a] The scaling expression used is $ET(10, n_2) = \Sigma_m \beta_m n_2^m$.
[b] The rows are indexed here by n_2 to show how the β change as ET(10, n_2) is added in the input set and the order of the polynomial is increased by one.

verification of the change in behaviour seen in fig. 2.) Above $n_2 = 8$. no accurate prediction is possible; the difference between the actual ET and that expected from extrapolation is substantial (table 3). Note however that the interpolation below $n_2 = 8$ is accurate: ET(10, 0) predicted from these data is in good agreement with that obtained from scaling the results for $\{n_1, 0\}$ levels at $E_k = 0.5$. At the higher kinetic energy, even this degree of accuracy vanishes: the coefficients in table 6 change erratically as more points are added, and no simple scaling form emerges.

3.2. Breakdown of the CST

It is clear from the results presented above that the inelastic collision behaviour of states $\{n_1, 0\}$ and $\{10, n_2\}$ is quite different. We therefore examine individual trajectories in more detail.

In the present collision case, since a large variety of initial states is studied at different kinetic energies, all the types of behaviour identified in fig. 1 can be observed. Three typical trajectories for initial state (10, 10) and $E_k = 2$ are shown in fig. 3 where we have graphed $R(t)$ and $E_0(t)$ versus time, and the trajectories are marked A, B and C (cf. fig. 1). To determine the intermediate internal motion, the trajectories are stopped at selected times during the collision, and the orbits allowed to develop in the absence of the collision potential. The PSS at such times for these trajectories are shown in fig. 4.

For the sequence $\{n_1, 0\}$ all trajectories examined were *only* of type A, i.e. the motion stayed regular throughout the collision. This is not surprising since the initial internal energy is well below E_c for all states, and at the kinetic energies of this study, the internal energy cannot exceed E_c. The orbits thus never sample regions of widespread chaos. Additionally, the initial tori $\Sigma_{n_1 0}$ are located in regions of great stability, and the collisions here do not sufficiently perturb this internal motion. (Since not every trajectory was examined at *all* intermediate times, it is possible that in some cases the orbits did pass through regions of limited chaos that occur below E_c.)

In contrast, many trajectories for levels in the $\{10, n_2\}$ sequence lead to chaotic final orbits, as

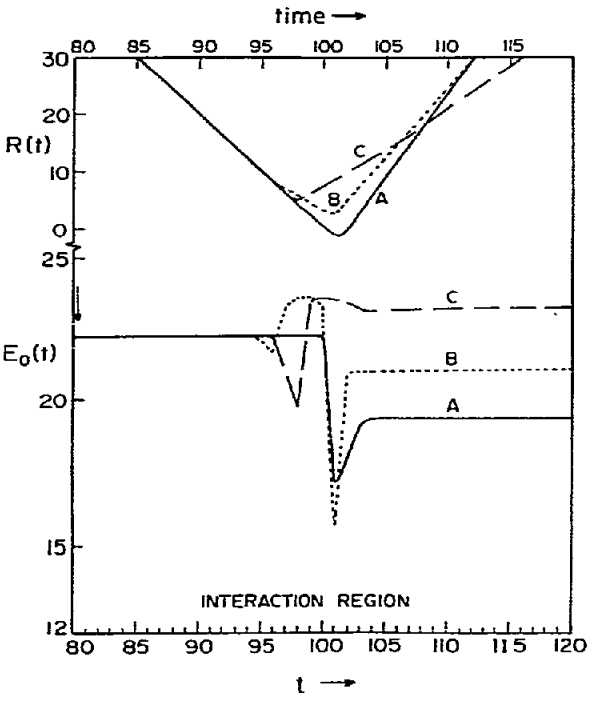

Fig. 3. Three typical trajectories for the collision of initial state $n_1 n_2 = 10$, 10 at $E_k = 2$. The internal energy, E_0 and the scattering coordinate are shown as a function of time, and are marked A, B and C with reference to fig. 1.

for example C in fig. 3. This occurs for all levels except $n_2 = 2$ at $E_k = 1$ and 2, and for $n_2 > 8$ at $E_k = 0.5$. Even when the final orbit is regular, in a majority of the cases, the orbits pass through chaotic regions (B in fig. 3); for these levels, the final state is invariably mixed. This is the *only* qualitative difference noticed in the trajectories for the two sequences, and it seems to be the reason for the quantitative differences in the ET variation.

When the internal motion is chaotic, the simple premises on which the CST is based [11,12] necessarily break down; the Taylor expansion and the perturbation theory which led [12] to the polynomial expression (6) is no longer valid.

Energy transfer in the presence of chaos can be enchanced [7] – either into the system or into translation – primarily due to the increased number of frequencies that are present in the vibrational motion. (In an earlier study [21] of atom–triatom collisions, an enhancement of the

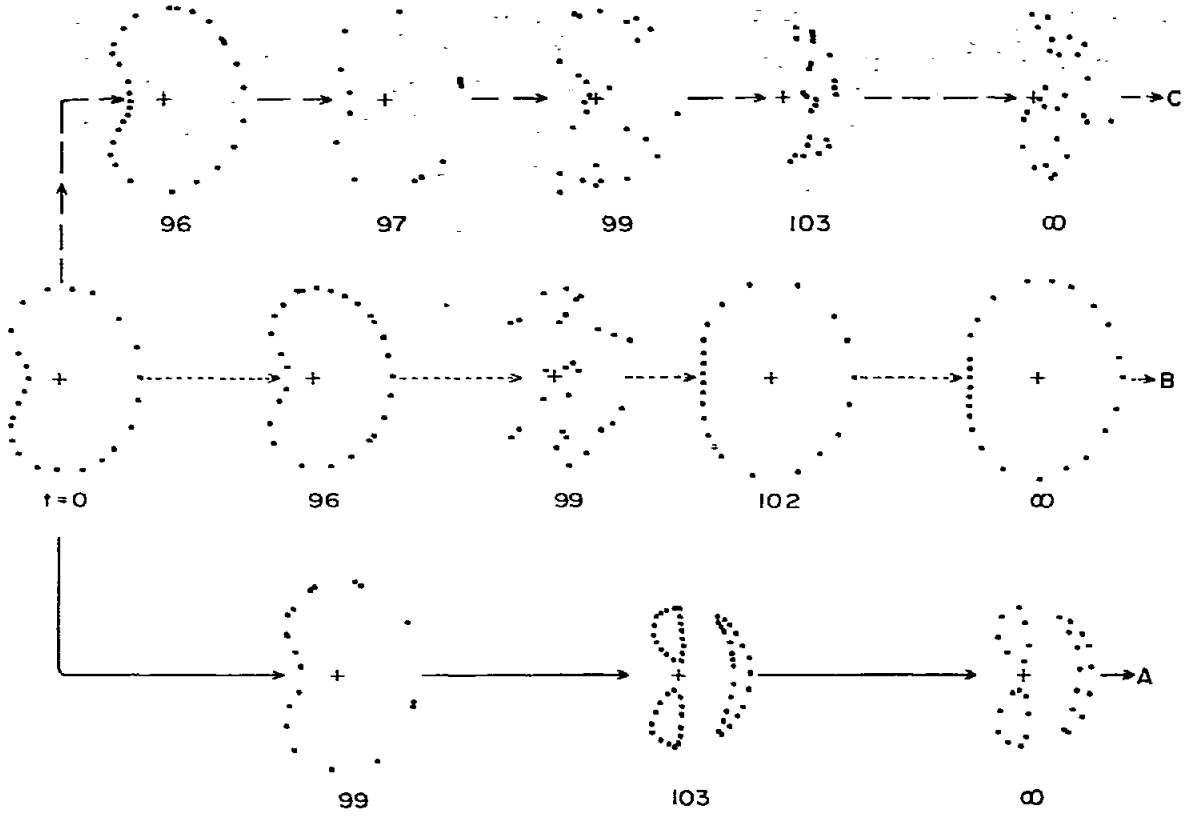

Fig. 4. Poincaré surfaces of section in the q_1-p_1 plane for internal motions along the trajectories in fig. 3. The + denotes the location of the origin and the numbers below the PSS indicate the particular time along the trajectory (marked in correspondence with figs. 1 and 3). The initial time is $t_0 = 0$.

ET with increasing initial vibrational excitation was observed, although no specific reference to the presence or role of chaotic motions was made there.) In one case, we see a *decrease* in the energy transferred into translation (V–T transfer): the exact ET for levels $n_2 = 10$ and 12 is smaller than that expected from the scaling in table 3. Such a decrease in the ET could be anticipated if energy transfer between the internal modes due to V–V processes becomes large [*].

[*] The (quantum) energy transfer moment from state n is $ET = \Sigma_m P_{nm}(\epsilon_m - \epsilon_n)$ where P_{nm} are the transition probabilities and ϵ_n is the energy of level n. When P_{nm} is large and $(\epsilon_m - \epsilon_n)$ is small, the overall ET will be smaller. Of course, the ET can be small for other reasons as well (e.g. when the elastic process dominates) so that the conclusion of enhanced V–V transfer from a reduction in the ET is not always justified.

As is well known [1,2,9,10] for systems such as (3), E_c is not a strict dividing line between regular and chaotic motions, but merely a rough guide as to when large-scale, widespread chaotic motions are likely. Thus at all energies lower than E_c, there are regions of limited chaos; above E_c there are regions of "vague tori" [7,20], i.e. motions that lie close to a torus for long times, but eventually (over some timescale τ) become chaotic. In either of these cases, the effect on the collision process is likely to be not very different from that of regular motions if the interaction time is relatively short compared to the timescale of the internal motion – the vibrational period. When the orbit is in such regions of "limited" chaos, if the collision complex is long-lived the interaction time may become longer than τ. Then the effect of such chaos on the collision should be substantial, and departures

from the scaling behaviour will be observable. The chaotic region is characterized by having a dense, continuous spectrum [1,2]; thus a wider range of frequencies is available for the interaction between the internal degrees of freedom and the translational mode. In addition, some features of the orbit motion can occur on timescales comparable to the interaction time (which can be shorter than the vibrational period). Consequently, when the trajectory encounters a region of widespread chaos directly, the effects are more pronounced, and departure from the scaling behaviour is seen even when the interaction time is relatively short.

It is useful to distinguish between those aspects of the collision that are due to the potential (4), and those intrinsic to such non-integrable molecular systems. For example, the fact that the ET is usually negative (energy is transferred into translation) is largely due to the exponential repulsion form of $V(R, q)$: with different forms of V, the ET can well be positive. Similarly, the single turning point in $R(t)$ is also a feature particular to this case. In the interaction region, the orbit can cycle back and forth between regular and chaotic regions (case B) regardless of the form of V; how often it does so is peculiar to the potential form and the kinetic energy. (Here, in all cases examined, this happened at most once per trajectory.) Finally, beyond the interaction region, the motion does not change in character; thus, if the orbit is regular (chaotic) at $R(t_2)$, it remains regular (chaotic) at $R = \infty$.

4. Discussion and summary

In this paper we have focused on the *variation* of collisional properties with initial action (or semiclassical state) in a simple non-integrable system. When the collision is such that the intermediate and final motion are regular, then we find that this variation is characterized by a simple polynomial dependence on the initial quantum number (or action), which then lends itself to accurate interpolation and extrapolation. However, when the intermediate or final motion is chaotic, then the character of the collision changes and the variation with initial state is no longer described by a simple polynomial form. Viewed in the context of the CST [11,12], therefore, there are substantial differences in the collision of non-integrable systems depending on whether regions of widespread chaos participate or not. (In order to employ the CST the initial actions must be well defined; in the present study, therefore, semiclassical states not associated with tori – the irregular levels [16] – cannot be considered.)

However, there is usually no a priori way in which one could predict if a particular collision will be influenced by chaos. This depends to a large extent on the location of the initial torus in the phase space of H_0, on the form of the interaction potential, and on the relative kinetic energy. In the present example, the tori for the sequence $\{n_1, 0\}$ are located deep in regions of stability, and the collisions tend to be de-exciting, and thus widespread chaotic motions do not play a role. All states of the sequence follow the CST. The $\{10, n_2\}$ states are located near regions of widespread chaos – this alone virtually ensures that sooner or later, some trajectories will lead the internal orbits through regions of chaos.

Given the proviso that one cannot ascertain beforehand whether chaotic internal motions will affect the collision process, there still are merits in using the CST in non-integrable systems evolving in such a way. When the CST applies, its utility here is at the least comparable to that in integrable systems [11–15]. It provides a means of data extension since the predictive accuracy is reasonable; this can greatly reduce computational effort. A extremely useful feature of the CST is that eq. (7) pertains to arbitrary actions I_1, I_2. The semiclassical quantization can be *entirely* bypassed if desired, since all that is required is that the ET for any given set of initial actions be known (thus it is not necessary to locate the particular semiclassical tori $\Sigma_{n_1 n_2}$ before studying the collision problem). The coefficients γ can be determined from the ET for arbitrary tori, and then used to generate the ET from any desired semiclassical level. (We have not used this procedure here since the primary concern was in establishing the validity of the CST, and further, the tori $\Sigma_{n_1 n_2}$ for this system are readily available.) This aspect of the CST is likely to be a great advantage in applications to molecu-

lar systems with several degrees of freedom wherein the semiclassical quantization itself can pose a difficulty [2].

Although applications here are to the first moment of the ET, the CST relates the change of any dynamical variable through equations analogous to (6). Higher-order moments typically require a larger number of terms in the expansion, and hence a larger set of input information. The major restriction is that we can only treat phase-averaged quantities (here initial-torus averages), so that state-to-state information is not easily accessible. This can only partially be circumvented: some connexions between the CST [11,12] and the quantum ECS scaling theory [22] for inelastic state-to-state quantities have been explored in an earlier article [14], where we have shown how the scaling coefficients can be interpreted in terms of quantum transition probabilities. The ECS theory has recently been successfully applied [23] to low-lying levels in an atom–(anharmonic) triatom collision system; it would therefore be of interest to determine where (and how) the theory fails for systems that reduce to a non-integrable hamiltonian in the classical limit, and whether there are any parallels with the present classical picture.

References

[1] S.A. Rice, Advan. Chem. Phys. 47 (1981) 117.
[2] D.W. Noid, M.L. Koszykowski and R.A. Marcus, Ann. Rev. Phys. Chem. 32 (1981) 267.
[3] D. Noid and M. Koszykowski, Chem. Phys. Letters 79 (1981) 485.
[4] G.C. Schatz, Chem. Phys. Letters 67 (1979) 248.
[5] G.C. Schatz and T. Mulloney, J. Chem. Phys. 71 (1979) 5257.
[6] D.W. Noid and W.-K. Liu, Chem. Phys. 62 (1981) 37.
[7] R.F. Nalewajski and R. Wyatt, Chem. Phys. 81 (1983) 357.
[8] D. Noid, M. Koszykowski, R.A. Marcus and J.D. McDonald, Chem. Phys. Letters 51 (1977) 540;
R. Ramaswamy, P.D. Siders and R.A. Marcus, J. Chem. Phys. 74 (1981) 4418;
K.D. Hänsel, Chem. Phys. Letters 57 (1978) 619;
D.L. Martin and R. Wyatt, Chem. Phys. 64 (1982) 203, and references therein.
[9] M.V. Berry, in: Nonlinear dynamics, AIP Conference Proceedings Ser. 46, ed. S. Jorna (AIP, Washington, 1978) p. 16.
[10] M. Tabor, Advan. Chem. Phys. 46 (1981) 73.
[11] A.E. DePristo, J. Chem. Phys. 75 (1981) 3384.
[12] R. Ramaswamy, J. Chem. Phys. 80 (1984) 2462.
[13] A.E. DePristo, J. Phys. Chem. 86 (1982) 1334.
[14] R. Ramaswamy and R. Bhargava, J. Chem. Phys. 80 (1984) 1095.
[15] R. Ramaswamy, Chem. Phys. 88 (1984) 7.
[16] I.C. Percival, Advan. Chem. Phys. 36 (1977) 1.
[17] K.S. Sorbie and N.C. Handy, Mol. Phys. 33 (1977) 1319.
[18] R.M. Stratt, N.C. Handy and W.H. Miller, J. Chem. Phys. 71 (1979) 3311.
[19] R. Ramaswamy and R.A. Marcus, J. Chem. Phys. 74 (1981) 1385.
[20] C. Jaffe and W.P. Reinhardt, J. Chem. Phys. 77 (1982) 5191.
[21] R. Dubrow and D.J. Wilson, J. Chem. Phys. 50 (1969) 1553.
[22] A.E. DePristo, S. Augustin, R. Ramaswamy and H. Rabitz, J. Chem. Phys. 71(1979) 850.
[23] D.C. Clary and A.E. De Pristo, J. Chem. Phys. 79 (1983) 2206.